

Acid wash experiments

Synapses were stimulated at the segmental nerve for 5 s at 50 Hz in 2.0 mM Ca²⁺ and imaged for 3 min before the HL3 saline (pH 7.0) in the bath was replaced with low pH acid wash (pH 5.5).

FM4-64 experiments

A total of 10 μM FM4-64 (Molecular Probes) was made in HL3 plus 0.5 mM Ca²⁺ saline and added to the bath. The nerve was stimulated for 1 min at 30 Hz. The synapse was then illuminated for 2 min. The preparation was washed repeatedly in Ca²⁺-free HL3 for 5 min, and an image of the synapse was captured. To analyse FM4-64 uptake the n-Syb-pH fluorescence in the green channel was used to define the region of interest, and the mean intensity of the fluorescence in the red channel defined by this region was calculated. We selected a small region of interest over the muscle background and the mean intensity of this region was subtracted from the synapse intensity to correct for variability in background FM4-64 levels.

shibire^{ts} experiments

Temperature was controlled by a heating/cooling stage with a Peltier module (Brook Industries) and monitored with a temperature probe in the imaging chamber. In Fig. 1d the nerve was stimulated identically (2 s, 50 Hz) at the permissive (22 °C) and restrictive temperatures (30 °C). In the FIAsh experiments (Fig. 2) we stimulated at the restrictive temperature (2 s, 50 Hz, in HL3) every 10 s for 200 s to deplete synaptic vesicles. After stimulation, the synapse was illuminated for 2 min. The chamber was then brought down to the permissive temperature. Images of the synapse were taken at about 2 min intervals after return to the permissive temperature, and the mean intensity of the synapse was measured at each time point.

Received 25 July; accepted 6 November 2003; doi:10.1038/nature02184.
Published online 23 November 2003.

1. Jarousse, N. & Kelly, R. B. Endocytotic mechanisms in synapses. *Curr. Opin. Cell Biol.* **13**, 461–469 (2001).
2. Fernandez-Chacon, R. *et al.* Synaptotagmin I functions as a calcium regulator of release probability. *Nature* **410**, 41–49 (2001).
3. Geppert, M. *et al.* Synaptotagmin I: a major Ca²⁺ sensor for transmitter release at a central synapse. *Cell* **79**, 717–727 (1994).
4. Littleton, J. T., Stern, M., Schulze, K., Perin, M. & Bellen, H. J. Mutational analysis of *Drosophila* synaptotagmin demonstrates its essential role in Ca(2+) -activated neurotransmitter release. *Cell* **74**, 1125–1134 (1993).
5. Perin, M. S., Fried, V. A., Mignery, G. A., Jahn, R. & Sudhof, T. C. Phospholipid binding by a synaptic vesicle protein homologous to the regulatory region of protein kinase C. *Nature* **345**, 260–263 (1990).
6. Brose, N., Petrenko, A. G., Sudhof, T. C. & Jahn, R. Synaptotagmin: a calcium sensor on the synaptic vesicle surface. *Science* **256**, 1021–1025 (1992).
7. Fergestad, T. & Broadie, K. Interaction of stoned and synaptotagmin in synaptic vesicle endocytosis. *J. Neurosci.* **21**, 1218–1227 (2001).
8. Jorgensen, E. M. *et al.* Defective recycling of synaptic vesicles in synaptotagmin mutants of *Caenorhabditis elegans*. *Nature* **378**, 196–199 (1995).
9. Littleton, J. T. *et al.* Synaptotagmin mutants reveal essential functions for the C2B domain in Ca²⁺-triggered fusion and recycling of synaptic vesicles *in vivo*. *J. Neurosci.* **21**, 1421–1433 (2001).
10. Reist, N. E. *et al.* Morphologically docked synaptic vesicles are reduced in synaptotagmin mutants of *Drosophila*. *J. Neurosci.* **18**, 7662–7673 (1998).
11. Jarousse, N. & Kelly, R. B. The AP2 binding site of synaptotagmin 1 is not an internalization signal but a regulator of endocytosis. *J. Cell Biol.* **154**, 857–866 (2001).
12. Zhang, J. Z., Davletov, B. A., Sudhof, T. C. & Anderson, R. G. Synaptotagmin I is a high affinity receptor for clathrin AP-2: implications for membrane recycling. *Cell* **78**, 751–760 (1994).
13. Haucke, V. & De Camilli, P. AP-2 recruitment to synaptotagmin stimulated by tyrosine-based endocytic motifs. *Science* **285**, 1268–1271 (1999).
14. Fukuda, M. *et al.* Role of the C2B domain of synaptotagmin in vesicular release and recycling as determined by specific antibody injection into the squid giant synapse preterminal. *Proc. Natl Acad. Sci. USA* **92**, 10708–10712 (1995).
15. Haucke, V., Wenk, M. R., Chapman, E. R., Farsad, K. & De Camilli, P. Dual interaction of synaptotagmin with mu2- and alpha-adaptin facilitates clathrin-coated pit nucleation. *EMBO J.* **19**, 6011–6019 (2000).
16. von Poser, C. *et al.* Synaptotagmin regulation of coated pit assembly. *J. Biol. Chem.* **275**, 30916–30924 (2000).
17. Sankaranarayanan, S. & Ryan, T. A. Real-time measurements of vesicle-SNARE recycling in synapses of the central nervous system. *Nature Cell Biol.* **2**, 197–204 (2000).
18. Sankaranarayanan, S. & Ryan, T. A. Calcium accelerates endocytosis of vSNAREs at hippocampal synapses. *Nature Neurosci.* **4**, 129–136 (2001).
19. Gandhi, S. P. & Stevens, C. F. Three modes of synaptic vesicular recycling revealed by single-vesicle imaging. *Nature* **423**, 607–613 (2003).
20. Miesenböck, G., De Angelis, D. A. & Rothman, J. E. Visualizing secretion and synaptic transmission with pH-sensitive green fluorescent proteins. *Nature* **394**, 192–195 (1998).
21. Koening, J. H. & Ikeda, K. Synaptic vesicles have two distinct recycling pathways. *J. Cell Biol.* **135**, 797–808 (1996).
22. Loewen, C. A., Mackler, J. M. & Reist, N. E. *Drosophila* synaptotagmin I null mutants survive to early adulthood. *Genesis* **31**, 30–36 (2001).
23. Yoshihara, M. & Littleton, J. T. Synaptotagmin I functions as a calcium sensor to synchronize neurotransmitter release. *Neuron* **36**, 897–908 (2002).
24. Marek, K. W. & Davis, G. W. Transgenically encoded protein photoinactivation (FIAsh-FALI): acute inactivation of synaptotagmin I. *Neuron* **36**, 805–813 (2002).
25. Griffin, B. A., Adams, S. R. & Tsien, R. Y. Specific covalent labeling of recombinant protein molecules inside live cells. *Science* **281**, 269–272 (1998).

26. Gaietta, G. *et al.* Multicolor and electron microscopic imaging of connexin trafficking. *Science* **296**, 503–507 (2002).
27. Kuromi, H. & Kidokoro, Y. Two distinct pools of synaptic vesicles in single presynaptic boutons in a temperature-sensitive *Drosophila* mutant, shibire. *Neuron* **20**, 917–925 (1998).
28. Aravanis, A. M., Pyle, J. L. & Tsien, R. W. Single synaptic vesicles fusing transiently and successively without loss of identity. *Nature* **423**, 643–647 (2003).
29. Verstreken, P. *et al.* Endophilin mutations block clathrin-mediated endocytosis but not neurotransmitter release. *Cell* **109**, 101–112 (2002).
30. Li, C. *et al.* Ca(2+) -dependent and -independent activities of neural and non-neural synaptotagmins. *Nature* **375**, 594–599 (1995).

Supplementary Information accompanies the paper on www.nature.com/nature.

Acknowledgements We thank M. Ramaswami and I. Robinson for *Drosophila* stocks, and D. DeAngelis, J. Rothman and R. Kelly for the supercliptic pHluorin GFP construct. We also thank E. Heckscher for comments on an earlier version of the manuscript.

Competing interests statement The authors declare that they have no competing financial interests.

Correspondence and requests for materials should be addressed to G.W.D. (gdavis@biochem.ucsf.edu).

.....

Lipid packing sensed by ArfGAP1 couples COPI coat disassembly to membrane bilayer curvature

Joëlle Bigay¹, Pierre Gounon², Sylviane Robineau¹ & Bruno Antony¹

¹Institut de Pharmacologie Moléculaire et Cellulaire, CNRS, 660 route des Lucioles, 06560 Valbonne-Sophia-Antipolis, France

²Centre Commun de Microscopie Appliquée, Université de Nice, Parc Valrose, 06103 Nice cedex 2, France

.....

Protein coats deform flat lipid membranes into buds and capture membrane proteins to form transport vesicles^{1–3}. The assembly/disassembly cycle of the COPI coat on Golgi membranes is coupled to the GTP/GDP cycle of the small G protein Arf1. At the heart of this coupling is the specific interaction of membrane-bound Arf1–GTP with coatamer, a complex of seven proteins that forms the building unit of the COPI coat^{4–7}. Although COPI coat disassembly requires the catalysis of GTP hydrolysis in Arf1 by a specific GTPase-activating protein (ArfGAP1)^{8–10}, the precise timing of this reaction during COPI vesicle formation is not known. Using time-resolved assays for COPI dynamics on liposomes of controlled size, we show that the rate of ArfGAP1-catalysed GTP hydrolysis in Arf1 and the rate of COPI disassembly increase over two orders of magnitude as the curvature of the lipid bilayer increases and approaches that of a typical transport vesicle. This leads to a model for COPI dynamics in which GTP hydrolysis in Arf1 is organized temporally and spatially according to the changes in lipid packing induced by the coat.

We reported previously that a fragment of ArfGAP1 (amino acids 1–257), which includes the catalytic zinc-finger domain, and Gcs1p, a yeast ArfGAP1 homologue, bind preferentially to liposomes containing conical lipids versus cylindrical lipids¹¹. The binding increased gradually as the size of lipid polar heads decreased and as the cross-section of the acyl chains increased. Because the marked preference of [1–257]ArfGAP1 for conical lipids correlated with its activity on liposome-bound Arf1–GTP¹¹, we suggested that a loose lipid packing favours the positioning of ArfGAP1 towards membrane-bound Arf1–GTP. Similar effects of the balance between conical and cylindrical lipids were observed

on the binding and the activity of full-length ArfGAP1 (data not shown).

Because the link between COPI vesicle biogenesis and lipid metabolism remains elusive^{12,13}, we reasoned that if lipid packing was at the root cause of the effects observed, changes in GAP activity should be observed by varying the liposome radius while keeping the lipid composition constant. This seemed promising in the context of COPI vesicle formation, because of the membrane distortions imposed by the coat during budding and notably the increase in lipid spacing in the coat-facing leaflet. Liposomes with a composition approaching that of Golgi membranes were prepared by sequential extrusions through 0.4, 0.2, 0.1 and 0.03 μm (pore size) polycarbonate filters¹⁴. We checked, using thin-layer chromatography and a phosphorus assay (Fig. 1a and data not shown), that the extrusion steps did not affect the lipid concentration and the composition of the liposomes. We assessed the size distribution of the liposomes by dynamic light scattering (Fig. 1b). To monitor the activity of full-length ArfGAP1 on liposome-bound Arf1-GTP, we took advantage of the large tryptophan fluorescence change that correlates with the transition of Arf1 between GTP- and GDP-bound forms¹¹. Strikingly, whereas liposome radius had no influence on Arf1 activation, a dramatic effect on the kinetics of Arf1 inactivation was observed (Fig. 1c; see also Supplementary Information). With large liposomes (hydrodynamic radius,

$R_h = 148 \pm 50 \text{ nm}$), the half-time of Arf1 inactivation initiated by the addition of 25 nM full-length ArfGAP1 was 306 s. As the liposome radius decreased, the half-time decreased to reach a value of 8 s with small liposomes ($R_h = 38 \pm 15 \text{ nm}$; Fig. 1d). Interestingly, the sensitivity to membrane curvature became very steep at radii approaching that of typical coated vesicles ($<50 \text{ nm}$). Because the ratio between ArfGAP1 and Arf in these experiments was 1:20, the rate constant for GTP hydrolysis on small ($R_h = 35\text{--}40 \text{ nm}$) liposomes was in the subsecond range ($k_{\text{cat}} > 1 \text{ s}^{-1}$).

The function of Arf proteins is not restricted to coated-vesicle formation and it was important to determine whether other Arf-GAP proteins, which are not involved in membrane trafficking, are sensitive to membrane curvature. We used a construct named PZA, derived from ASAP1, a protein involved in actin rearrangements^{15,16}. PZA consists of a PH domain, which binds phosphatidylinositol biphosphate, a zinc-finger 'GAP' domain homologous to the catalytic domain of ArfGAP1, and ankyrin repeats. Although PZA-catalysed GTP hydrolysis in Arf1 clearly occurred on the liposome surface, as demonstrated by the effect of phosphatidylinositol biphosphate, the activity of PZA was insensitive to liposome radius (Fig. 1e, f).

Next, we wished to determine whether membrane curvature directly influences the rate of COPI coat disassembly. Previous biochemical and electron microscopy studies have demonstrated that stable COPI-like coated vesicles can form when large liposomes are incubated with Arf1, coatmer and a non-hydrolysable GTP analogue^{17,18}. To monitor the assembly/disassembly cycle of the COPI coat in this minimal system, we used a light-scattering assay developed to study the dynamics of the COPII coat¹⁹. Briefly, the intensity of the light scattered by liposomes increased as the small G protein and the COP complexes are recruited to the lipid surface. Conversely, when the proteins dissociate, the intensity diminishes. In a first set of experiments, we used relatively large liposomes ($R_h = 150 \text{ nm}$) containing 2 mol% of a lipopeptide that imitates the cytosolic tail of the membrane protein p23 and favours coatmer recruitment¹⁸. In Fig. 2a, the order of additions follows the established order of events in COPI assembly and disassembly. Arf1-GDP was first activated by the addition of GTP and by lowering temporarily the free Mg^{2+} concentration from 1 mM to 1 μM with EDTA. During this stage, a small light-scattering increase was observed, which correlated with the GDP/GTP exchange reaction as monitored by tryptophan fluorescence (data not shown). The subsequent addition of coatmer induced a large and instantaneous light-scattering increase. Last, upon the addition of a catalytic amount of ArfGAP1 the signal returned to the initial level within a few minutes. Inverting the order of protein additions (Fig. 2b) or replacing GTP by $\text{GTP}\gamma\text{S}$, a non-hydrolysable analogue (Fig. 2c), demonstrated that these three signals correspond respectively to Arf recruitment, coatmer recruitment and ArfGAP1-induced COPI disassembly.

The rate of ArfGAP1-induced COPI disassembly as monitored by light-scattering (Fig. 2a, continuous trace) was faster than the rate of ArfGAP1-catalysed GTP hydrolysis on isolated Arf1, as monitored by fluorescence (Fig. 2a, dashed trace). Several factors could account for this difference. First, coatmer and p23 proteins could modulate ArfGAP1 activity²⁰. In addition, COPI-induced membrane bending could increase ArfGAP1 activity. We visualized, using electron microscopy, the membrane deformations induced by the COPI coat before the addition of ArfGAP1 (Fig. 2d). In agreement with ref. 18, COPI-coated vesicles clearly bud off from some liposomes. Yet, COPI-coated membranes with a clear budding profile and small ($<100 \text{ nm}$) COPI-like coated vesicles constituted no more than 15% of the total surface of COPI-coated membranes. Therefore the rate of COPI coat disassembly measured in Fig. 2a essentially reflects the dynamics of weakly curved coated profiles.

To determine unambiguously the effect of membrane curvature

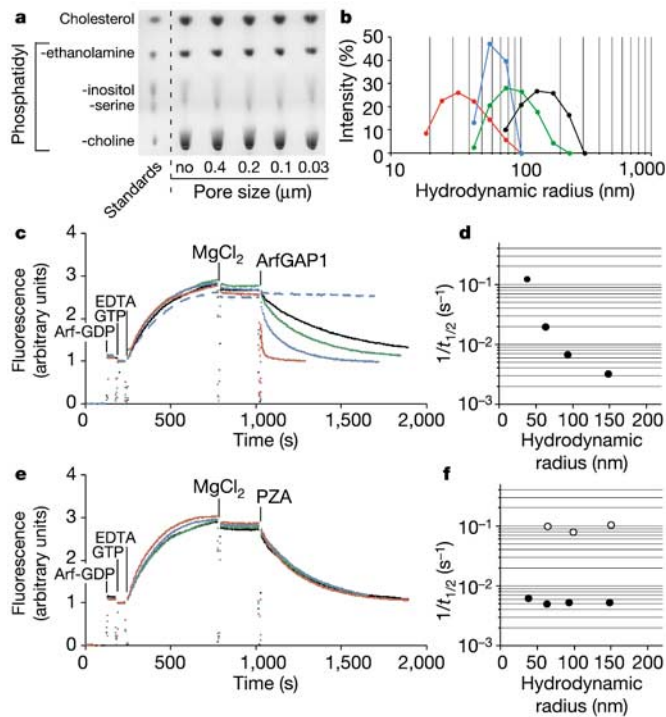


Figure 1 Membrane curvature increases ArfGAP1 activity. **a**, Thin-layer chromatography of Golgi-like liposomes prepared by sequential extrusion through polycarbonate filters of decreasing pore size. **b**, Radius distribution of the extruded liposomes as determined by dynamic light scattering. Pore size in μm : 0.4 (black), 0.2 (green), 0.1 (blue) and 0.03 (red). **c**, Tryptophan fluorescence measurements of the GDP/GTP cycle of Arf1 (0.5 μM) on the liposomes characterized in **a** and **b**. Arf1 was activated by the addition of GTP (100 μM) and by lowering the concentration of Mg^{2+} with EDTA. Inactivation was initiated by the addition of ArfGAP1 (25 nM). Dashed trace: control with $\text{GTP}\gamma\text{S}$. **d**, Rate ($1/t_{1/2}$) of ArfGAP1-catalysed GTP hydrolysis as a function of the mean hydrodynamic radius (R_h). **e**, **f**, Control experiments with PZA (25 nM). Time courses and black circles represent standard liposomes; white circles represent standard liposomes supplemented with 2% phosphatidylinositol biphosphate.

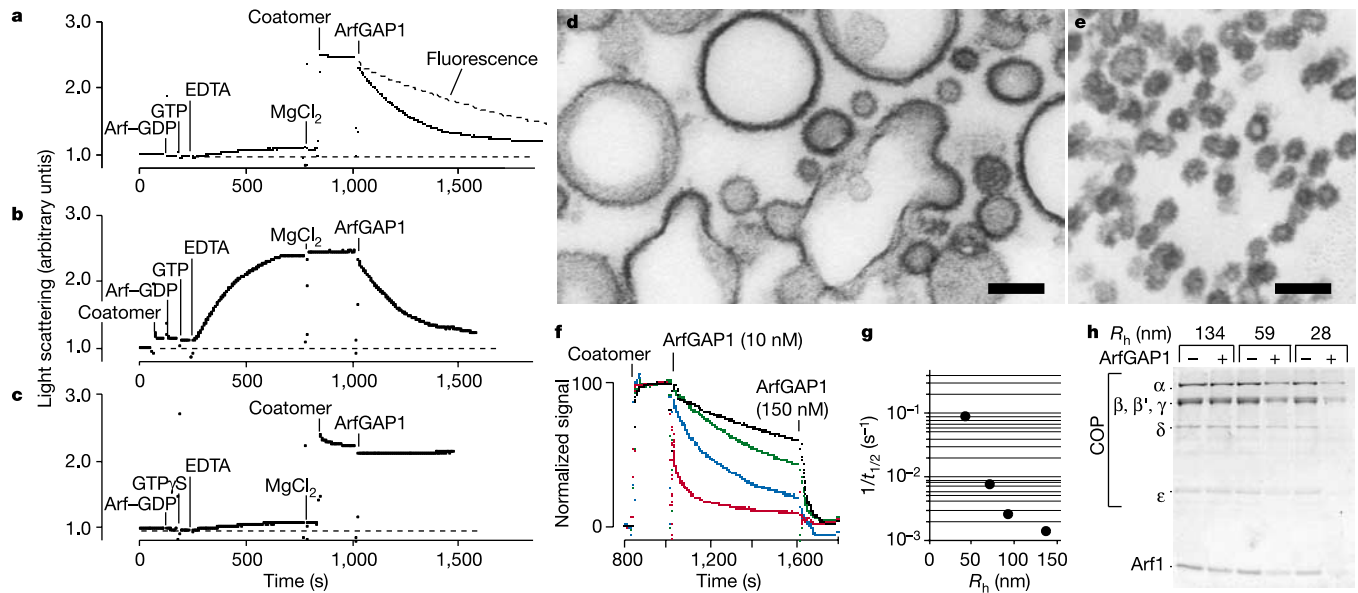


Figure 2 Membrane curvature increases the rate of COPI disassembly. **a–c**, Assembly–disassembly cycle of the COPI coat on large liposomes ($R_h = 150$ nm; p23 lipopeptide: 2%). Arf1–GDP (0.5 μ M), nucleotide (100 μ M), coatamer (0.15 μ M) and ArfGAP1 (25 nM) were added to the liposome suspension as indicated. The scattering of light was measured continuously. The dashed trace reports the time course of Arf1 inactivation as measured by tryptophan fluorescence in the absence of coatamer and lipopeptide.

d, e, Coated profiles observed by electron microscopy on large (**d**, $R_h = 145$ nm) or small (**e**, $R_h = 31$ nm) liposomes after incubation with Arf1, GTP and coatamer before the addition of ArfGAP1. Scale bar, 100 nm. **f**, Same as in **a** with liposomes of decreasing radius (same colour code as in Fig. 1). **g**, Rate ($1/t_{1/2}$) of COPI disassembly as a function of liposome hydrodynamic radius. **h**, Sedimentation analysis of liposome-bound proteins before (–) and 1 min after (+) the addition of 10 nM ArfGAP1.

on COPI dynamics, the light-scattering assay shown in Fig. 2a was repeated with liposomes of decreasing radius. Figure 2e shows an example of small ($R_h = 31$ nm) liposomes covered with the COPI coat. Figure 2f and g shows that the rate of COPI coat disassembly increased over two orders of magnitude as the liposome radius decreased. Thus, whereas the COPI coat associated with large liposomes ($R_h = 140$ nm) was quite resistant to ArfGAP1 ($t_{1/2} = 700$ s), it dissociated from small liposomes ($R_h = 35$ nm) within a few seconds ($t_{1/2} = 11$ s) once a catalytic amount of ArfGAP1 was added. Again, the sensitivity to membrane curvature was very high at low radii (Fig. 2g). These findings were

confirmed by sedimentation experiments in which liposome-bound proteins were analysed before and after the addition of ArfGAP1 (Fig. 2h).

Ionic complexes between fluoride and aluminium (AlF_x) can imitate a γ -phosphate group en route for hydrolysis²¹. For small G proteins, the binding of AlF_x requires the catalytic machinery provided by a GAP protein²². AlF_x promotes the formation of COPI-coated-vesicles, but the molecular basis for this effect is not known^{4,23}. We reasoned that if the effect of AlF_x on COPI relies on the stabilization of an interaction of Arf1–GDP with AlF_x and ArfGAP1, and if this interaction depends on membrane curvature, one may observe an effect of AlF_x on reconstituted COPI reactions performed with small liposomes. Coatamer, ArfGAP1 and Arf1–GDP were added to liposomes of decreasing radius in the presence or in the absence of AlF_x . At the end of the experiments, GTP γ S and

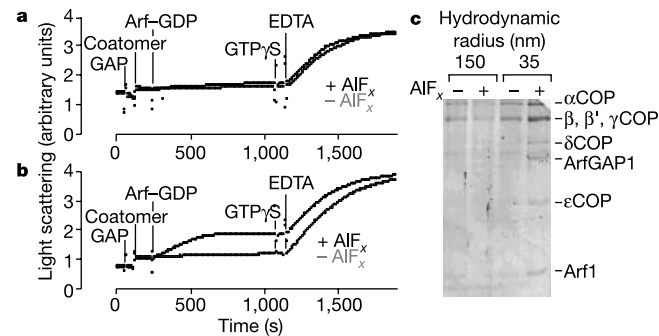


Figure 3 Membrane curvature facilitates the co-assembly of Arf1–GDP with ArfGAP1 and coatamer in the presence of AlF_x . **a**, Light-scattering measurements on large liposomes ($R_h = 150$ nm) with (black trace) or without (grey trace) 8 mM KF and 400 μ M $AlCl_3$. ArfGAP1 (0.5 μ M), coatamer (0.3 μ M) and Arf1–GDP (1 μ M) were sequentially added. **b**, Same as in **a** with small liposomes ($R_h = 35$ nm). **c**, Sedimentation analysis. Experiments similar to that shown in **a** and **b** were performed except that no GTP γ S was added. At time = 1,100 s, the samples were centrifuged and the pellets were analysed by SDS–PAGE.

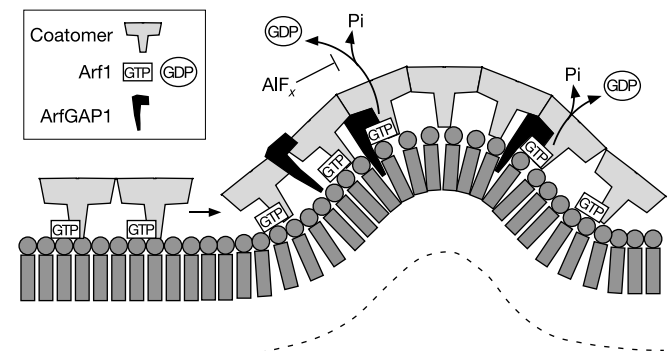


Figure 4 Model for the temporal and spatial distribution of ArfGAP1-catalysed GTP hydrolysis in Arf1 during the formation of a COPI bud. For simplicity, the interaction of the COPI machinery with membrane proteins, which could also influence the rate of GTP hydrolysis, is not shown. Pi, inorganic phosphate.

EDTA were added to provide a reference for the maximal binding signal. On large liposomes supplemented with 2% p23 lipopeptide, the light-scattering recordings with or without Alf_x were almost indistinguishable and no binding signal was observed before the addition of $GTP\gamma S$ (Fig. 3a, c). In contrast, an Alf_x -dependent signal was detected on small liposomes (Fig. 3b, c). Importantly, whatever the order of protein additions used, the Alf_x -dependent signal was observed after the third protein addition (for example, Arf1-GDP in Fig. 3b), suggesting that Alf_x stabilizes a ternary complex between Arf1-GDP, ArfGAP1 and coatomer provided that the supporting bilayer is sufficiently bent. We note that Arf1 concentrates in buds compared with flat Golgi cisternae in the presence of Alf_x (ref. 4). In conclusion, the effect of Alf_x suggests that the adjustment of the enzymatic machinery that drives GTP hydrolysis in COPI is governed at a distance by the penetration of ArfGAP1 into the coat-facing leaflet as the membrane becomes curved.

The remarkable sensitivity of ArfGAP1 to membrane curvature determines a spatial and temporal programme for GTP hydrolysis in a COPI bud (Fig. 4). As a polymerized COPI coat increases membrane curvature, the number of Arf1-GTP molecules that hold the coat should decrease dramatically. In line with what has been proposed for other coats^{24,25}, this decrease is probably compensated by an increase in the lateral interactions between COP proteins as the coat lattice becomes spherical. Furthermore, because membrane curvature at the periphery of the coated area is negative, a ring of Arf1-GTP molecules should be protected from ArfGAP1 and may keep the coat in a metastable state, ready to disassemble as soon as membrane fission occurs (when membrane curvature becomes entirely positive). Overall, such a mechanism would explain why the release of Arf1 from Golgi membranes is faster than the release of coatomer and that vesicles with an unstable coat and with a low Arf1/coatomer ratio form in the presence of ArfGAP1 and $GTP^{26,27}$. □

Methods

Proteins

Arf1 was coexpressed in *Escherichia coli* with N-myristoylated-transferase and the myristoylated form was purified as described²⁸. Rabbit-liver coatomer was purified as described²⁹ and further purified by gel-filtration on a Sephacryl S-300 column. Full length ArfGAP1 with a carboxy-terminal hexahistidine tag was purified from Sf9 cells by nickel and mono-Q chromatography.

Liposomes

Liposomes were prepared by extrusion through polycarbonate filters¹⁴. The composition was 50 mol% egg phosphatidylcholine, 19% liver phosphatidylethanolamine, 5% brain phosphatidylserine, 10% liver phosphatidylinositol and 16% cholesterol. When indicated, 2% phosphatidylinositol bisphosphate was added at the expense of phosphatidylinositol. To check that the lipid composition remained constant throughout the sequential extrusion protocol, the liposomes were analysed by thin-layer chromatography using a chloroform/methanol/water/acetic acid (60:50:4:1) solvent system. Lipids were detected by iodine. The p23 lipopeptide was synthesized and purified as described²⁹ and added from a stock solution in DMSO to the extruded liposomes to give a final surface concentration of 2 mol lipopeptide/100 mol exposed lipid.

Dynamic light scattering

The hydrodynamic radius of the extruded liposomes was assessed by dynamic light scattering using a Dynapro MSX instrument at a final lipid concentration of 0.1 mM.

Tryptophan fluorescence and static light-scattering measurements

All experiments were performed at 37 °C. The buffer used was HEPES 50 mM, pH 7.2, potassium acetate 120 mM, $MgCl_2$ 1 mM, DTT 1 mM. The final lipid concentration was 0.2 mM (fluorescence) or 0.1 mM (light scattering). Tryptophan fluorescence (excitation, 297.5 nm; emission, 340 nm) and light scattering (350 nm) were measured in a small quartz cuvette (volume, 100 μ l) at right angles. The kinetics of ArfGAP1-catalysed GTP hydrolysis on Arf1 and the kinetics of COPI disassembly could not be fitted by a single exponential function (this probably reflects the heterogeneity in size of the liposomes). We determined graphically the apparent half-time ($t_{1/2}$) and used $1/t_{1/2}$ as a rate unit.

Sedimentation

Liposomes and proteins were incubated in small polycarbonate tubes under the same conditions as that used for the light-scattering experiments. The samples were centrifuged

at 50,000g for 15 min at 25 °C and the pellets were analysed by SDS-polyacrylamide gel electrophoresis (PAGE) with Sypro orange staining.

Electron microscopy

Samples from light scattering experiments were collected, fixed with 2% glutaraldehyde, centrifuged at 100,000g for 30 min and the pellet was then processed for electron microscopy as described³⁰.

Received 27 June; accepted 7 October 2003; doi:10.1038/nature02108.

- Rothman, J. E. & Wieland, F. T. Protein sorting by transport vesicles. *Science* **272**, 227–234 (1996).
- Schekman, R. & Orci, L. Coat proteins and vesicle budding. *Science* **271**, 1526–1533 (1996).
- Kirchhausen, T. Three ways to make a vesicle. *Nature Rev. Mol. Cell Biol.* **1**, 187–198 (2000).
- Serafini, T. *et al.* ADP-ribosylation factor is a subunit of the coat of Golgi-derived COP-coated vesicles: a novel role for a GTP-binding protein. *Cell* **67**, 239–253 (1991).
- Donaldson, J. G., Cassel, D., Kahn, R. A. & Klausner, R. D. ADP-ribosylation factor, a small GTP-binding protein, is required for binding of the coatomer protein beta-COP to Golgi membranes. *Proc. Natl Acad. Sci. USA* **89**, 6408–6412 (1992).
- Orci, L., Palmer, D. J., Amherdt, M. & Rothman, J. E. Coated vesicle assembly in the Golgi requires only coatomer and ARF proteins from the cytosol. *Nature* **364**, 732–734 (1993).
- Zhao, L. *et al.* Direct and GTP-dependent interaction of ADP ribosylation factor 1 with coatomer subunit beta. *Proc. Natl Acad. Sci. USA* **94**, 4418–4423 (1997).
- Tanigawa, G. *et al.* Hydrolysis of bound GTP by ARF protein triggers uncoating of Golgi-derived COP-coated vesicles. *J. Cell Biol.* **123**, 1365–1371 (1993).
- Cukierman, E., Huber, I., Rotman, M. & Cassel, D. The ARF1 GTPase-activating protein: zinc finger motif and Golgi complex localization. *Science* **270**, 1999–2002 (1995).
- Reinhard, C., Schweikert, M., Wieland, F. T. & Nickel, W. Functional reconstitution of COPI coat assembly and disassembly using chemically defined components. *Proc. Natl Acad. Sci. USA* **100**, 8253–8257 (2003).
- Antony, B., Huber, I., Paris, S., Chabre, M. & Cassel, D. Activation of ADP-ribosylation factor 1 GTPase-activating protein by phosphatidylcholine-derived diacylglycerols. *J. Biol. Chem.* **272**, 30848–30851 (1997).
- Stammes, M., Schiavo, G., Stenbeck, G., Sollner, T. H. & Rothman, J. E. ADP-ribosylation factor and phosphatidic acid levels in Golgi membranes during budding of coatomer-coated vesicles. *Proc. Natl Acad. Sci. USA* **95**, 13676–13680 (1998).
- Yanagisawa, L. L. *et al.* Activity of specific lipid-regulated ADP ribosylation factor-GTPase-activating proteins is required for Sec14p-dependent Golgi secretory function in yeast. *Mol. Biol. Cell* **13**, 2193–2206 (2002).
- Mayer, L. D., Hope, M. J. & Cullis, P. R. Vesicles of variable sizes produced by a rapid extrusion procedure. *Biochim. Biophys. Acta* **858**, 161–168 (1986).
- Brown, M. T. *et al.* ASAP1, a phospholipid-dependent arf GTPase-activating protein that associates with and is phosphorylated by Src. *Mol. Cell Biol.* **18**, 7038–7051 (1998).
- Randazzo, P. A. *et al.* The Arf GTPase-activating protein ASAP1 regulates the actin cytoskeleton. *Proc. Natl Acad. Sci. USA* **97**, 4011–4016 (2000).
- Spang, A., Matsuoka, K., Hamamoto, S., Schekman, R. & Orci, L. Coatomer, Arf1p, and nucleotide are required to bud coat protein complex I-coated vesicles from large synthetic liposomes. *Proc. Natl Acad. Sci. USA* **95**, 11199–11204 (1998).
- Bremser, M. *et al.* Coupling of coat assembly and vesicle budding to packaging of putative cargo receptors. *Cell* **96**, 495–506 (1999).
- Antony, B., Madden, D., Hamamoto, S., Orci, L. & Schekman, R. Dynamics of the COPII coat with GTP and stable analogues. *Nature Cell Biol.* **3**, 531–537 (2001).
- Goldberg, J. Decoding of sorting signals by coatomer through a GTPase switch in the COPII coat complex. *Cell* **100**, 671–679 (2000).
- Chabre, M. Aluminofluoride and berylliofluoride complexes: new phosphate analogs in enzymology. *Trends Biochem. Sci.* **15**, 6–10 (1990).
- Scheffzek, K., Ahmadian, M. R. & Wittinghofer, A. GTPase-activating proteins: helping hands to complement an active site. *Trends Biochem. Sci.* **23**, 257–262 (1998).
- Finazzi, D., Cassel, D., Donaldson, J. G. & Klausner, R. D. Aluminum fluoride acts on the reversibility of ARF1-dependent coat protein binding to Golgi membranes. *J. Biol. Chem.* **269**, 13325–13330 (1994).
- Zhu, Y., Traub, L. M. & Kornfeld, S. ADP-ribosylation factor 1 transiently activates high-affinity adaptor protein complex AP-1 binding sites on Golgi membranes. *Mol. Biol. Cell* **9**, 1323–1337 (1998).
- Antony, B., Gounon, P., Schekman, R. & Orci, L. Self-assembly of minimal COPII cages. *EMBO Rep.* **4**, 419–424 (2003).
- Presley, J. F. *et al.* Dissection of COPI and Arf1 dynamics *in vivo* and role in Golgi membrane transport. *Nature* **417**, 187–193 (2002).
- Yang, J. S. *et al.* ARFGAP1 promotes the formation of COPI vesicles, suggesting function as a component of the coat. *J. Cell Biol.* **159**, 69–78 (2002).
- Franco, M., Chardin, P., Chabre, M. & Paris, S. Myristoylation of ADP-ribosylation factor 1 facilitates nucleotide exchange at physiological Mg^{2+} levels. *J. Biol. Chem.* **270**, 1337–1341 (1995).
- Nickel, W. & Wieland, F. T. Receptor-dependent formation of COPI-coated vesicles from chemically defined donor liposomes. *Methods Enzymol.* **329**, 388–404 (2001).
- Matsuoka, K. & Schekman, R. The use of liposomes to study COPII- and COPI-coated vesicle formation and membrane protein sorting. *Methods* **20**, 417–428 (2000).

Supplementary Information accompanies the paper on www.nature.com/nature.

Acknowledgements We thank P. Randazzo and R. Premont for proteins and constructs, J. Moelleken for advice on coatomer purification and lipopeptide synthesis and M. Chabre for discussions. This work was supported by the CNRS (ACI 'Jeune Chercheur') and the EMBO Young Investigator Programme.

Competing interests statement The authors declare that they have no competing financial interests.

Correspondence and requests for materials should be addressed to B.A. (antony@ipmc.cnrs.fr).